Research Square

Preprints are preliminary reports that have not undergone peer review.
They should not be considered conclusive, used to inform clinical practice,
or referenced by the media as validated information.

A New Flexible Inverted Exponential Distribution: Characterization, Distinct Estimations and Applications

Hadil Alhazmi
Princess Nourah bint Abdulrahman University
Akeem Ajibola Adepoju
akeebola@kustwudil.edu.ng

Aliko Dangote University of Science and Technology
Abdulmumeen Adekunle Issa
Abubakar Tafawa Balewa University
Bello Olalekan Akanji
Osun State University
Zahrah Fayez Althobaiti
University of Tabuk

Article

Keywords: Inverted Exponential distribution, Type I Half Logistic Topp-Leone family, Parameter estimation, L-moments, Energy distance estimation

Posted Date: November 12th, 2026

DOI: https://doi.org/10.21203/rs.3.rs-11195976/v1

License: This work is licensed under a Creative Commons Attribution 4.0 International License.
Read Full License

Additional Declarations: No competing interests reported.

A New Flexible Inverted Exponential Distribution: Characterization, Distinct Estimations and Applications

Hadil Alhazmi[1], Akeem Ajibola Adepoju[2], Abdulmumeen Adekunle Issa[3], Bello Olalekan Akanji[4], Zahrah Fayez Althobaiti[5]

[1]Department of Mathematical Sciences, College of Science, Princess Nourah Bint Abdulrahman University, P.O. Box 84428, Riyadh 11671, Saudi Arabia, [2]Department of Statistics, Aliko Dangote University of Sceince and Technology, Wudil, 713281, Kano. Nigeria. [3]Department of Statistics, Abubakar Tafawa Balewa University. Bauchi. Nigeria. [4]Department of Statistics, Osun State University Osogbo. Nigeria. [5]Department of Statistics, Faculty of Science, University of Tabuk, 71491, Tabuk, Saudi Arabia.

Correspondence: Akeem Ajibola Adepoju orcid 0000-0003-1376-7369 (akeebola@gmail.com, akeebola@kustwudil.edu.ng)

Keywords: Inverted Exponential distribution; Type I Half Logistic Topp-Leone family; Parameter estimation; L-moments; Energy distance estimation.

Abstract

The study introduces a new probability distribution through integrating the Inverted Exponential distribution with the Type I Half Logistic Topp-Leone family of distributions. The resulting distribution, named; the Type I Half Logistic Topp-Leone Inverted Exponential Distribution (TIHLTLIE), avails the research environment with a new flexible framework for addressing diverse reliability and lifetime modeling. Several important mathematical properties of the proposed distribution, including moments (Ms), probability weighted moments (PWMs), and the moment generating function (MGF), are tractably obtained. Key reliability characteristics such as the hazard rate function, survival function and quantile function are derived and graphically visualized to demonstrate the behavior of the distribution. Parameter estimation is examined extensively through a comprehensive number of estimation approaches, namely, the Maximum Likelihood Estimation (MLE), Maximum Product of Spacings (MPS), Least Squares (LS), Weighted Least Squares (WLS), Cramér–von Mises (CVM), Anderson–Darling (AD), Percentile Estimation (PE), Method of Moments (MOM), L-Moments (L-MOM), Probability Weighted Moments (PWM), Trimmed L-Moments (TL-MOM), Wasserstein Distance Estimation (WDE), and Energy Distance Estimation (ENE). Rigorous Monte Carlo simulation study is performed to investigate the efficiency and consistency of these techniques via distinct sample sizes. The results demonstrate the performance exhibited in term of estimation accuracy across various scenarios by distance- and moment-based approaches,

particularly the Energy Distance and L-moment-related estimators is superb. Finally, the applicability of the TIHLTLIE distribution is illustrated using two real-world datasets, where it provides a better fit than several comparators according to various information criteria. These findings demonstrate the applicability of the proposed distribution as a versatile distribution for modeling positively skewed data encountered in lifetime datasets.

1 | Introduction

Several real-world studies, classical probability distributions (CPDs) often fail to provide an adequate fit for complex phenomena. As noted in the literature [1,2], no single CPD possesses the versatility to consistently and effectively model all types of datasets. Consequently, extension of existing CPDs by integrating more parameters to strengthen their applicability, flexibility, and goodness-of-fit remains crucial goal in statistical study [3]. The development of new probability distributions with improved structural flexibility maintains its risen relevant, especially using generalized families of distributions (GFDs). The applications of the GFD across diverse studies, such as medicine, psychology, economics, finance, biology, actuarial science, engineering, geology, and environmental science.

Exponential distribution stands-out among the commonly explored CPD, often considered for its simplicity property, akin to the Geometric distribution. However, its constant hazard rate assumption weakened its effectiveness, specifically for modeling lifetimes demonstrating non-monotonic hazard functions such as the inverted-bathtub and bathtub shapes. To address these limitations, studies [4], [5], [6], [7], [8] have introduced improved version of the classical Exponential distribution. For instance, [9] employed different classical estimation approached for its generalized of the classical exponential distribution.

The Inverted Exponential (IE) distribution, being an improved version of the Exponential distribution, was introduced to overcome the constant hazard rate limitation [10]. Despite the fact that the IE distribution is a useful lifetime distribution and a special case of the Inverted Weibull distribution that exhibits capability of modeling data that present inverted bathtub failure rates, its usefulness is still limited due to its constraint in handling high skewness and heavy tailed data. Many studies such as [11], [12], [13], [14], [15], had extend the IE distribution. Even though, the extension of classical distribution is not limited to IE distribution alone, studies by [16], [17], [18], [19], [20],[22], [23], [24] and [25] further iterate the important of extending the classical distributions..

The Type I Half Logistic Topp-Leone-G (TIHLTL-G) family of distributions, introduced by [5] Is a notable advancement in distribution studies. This family introduces two shape parameters capable of extending classical distributions, significantly increasing their flexibility through the skewedness and tailed capacity. The TIHLTL-G family has been successfully applied in medical research, for instance, cancer studies and environmental modeling (rainfall data), demonstrating superior performance and adaptability.

In other scenarios, datasets with constant hazard rates are rare. Often electronics and mechanical systems exhibit failure rate that demonstrate non-constant monotonous hazard rates, which makes flexible lifetime modeling important in reliability engineering [14], hence the quest for distributions extension.

Going forward, this study introduces a new extension of the Inverted Exponential distribution termed the Type I Half Logistic Topp-Leone Inverted Exponential (TIHLTLIE) distribution. This new

distribution incorporates two extra positive shape parameters into the IE distribution, thereby improve the modified distribution capacity to model a wider variety of data with improved fitting ability.
The major motivations for this extension are as follows:

- To augment the flexibility of the IE distribution with additional new shape parameters;
- To provide greater adaptability for modeling complex failure rate structures;
- To examined the model parameter behavior using extensive methods of estimation
- To develop a model that demonstrates consistent and superior performance compared to existing alternatives.

The primary objective of this study is to introduce and investigate the statistical properties, inferences procedures, and practical applications of the TIHLTLIE distribution. The remaining part of this article is structured as follows:

- Section 2 presents the formulation of the TIHLTLIE distribution along with its probability functions and statistical properties.
- Section 3 addresses parameter estimation using the MLE, MPS, LS, WLS, CVM, PE, MOM, L_MOM, PWM, WDE, TL-MOM and ENE methods.
- Section 4 provides a simulation study to evaluate the performance of the estimators.
- Section 5 applies the proposed model to two real datasets and compares its performance to existing competing models, including the Topp-Leone Odd Log-Logistic Inverted Exponential (TLOLL-IE), Gompertz Inverse Exponential (Go-IE), and Weighted Weibull Inverse Exponential (WW-IE) distributions.

2 | Formulation of the New Model

Suppose the cdf and pdf of the Type I Half Logistic Topp-leone-G family of distribution is expressed as

$$F_{TIHLTL-G}\left(t;\zeta,\beta,\gamma\right)=\frac{1-\left[1-\left[1-\left[1-F\left(t;\gamma\right)\right]^2\right]^\beta\right]^\zeta}{1+\left[1-\left[1-\left[1-F\left(t;\gamma\right)\right]^2\right]^\beta\right]^\zeta}, \tag{1}$$

$$f_{TIHLTL-G}\left(t;\zeta,\beta,\gamma\right)=\frac{4\zeta\beta f\left(t;\gamma\right)\left[1-F\left(t;\gamma\right)\right]\left[1-\left[1-F\left(t;\gamma\right)\right]^2\right]^{\beta-1}\left[1-\left[1-\left[1-F\left(t;\gamma\right)\right]^2\right]^\beta\right]^{\zeta-1}}{\left[1+\left[1-\left[1-\left[1-F\left(x;\gamma\right)\right]^2\right]^\beta\right]^\zeta\right]^2}, \tag{2}$$

In this context, b and z represent the shape parameters, and g corresponds to the parameter vector of the baseline Inverted Exponential distribution.

Now, consider the Inverted Exponential distribution with CDF and PDF below:

$$F\left(t;\alpha\right)=e^{-\left(\frac{\alpha}{t}\right)} \tag{3}$$

$$f\left(t;\alpha\right)=\frac{\alpha}{t^2}e^{-\left(\frac{\alpha}{t}\right)} \tag{4}$$

The TIHLTLIE model is introduced as a new generalization. A random variable t is said to be distributed according to TIHLTLIE if its CDF is defined by Equation (5).

$$F_{TIHLTLIE}\left(t;\zeta,\beta,\alpha\right)=\frac{1-\left[1-\left[1-\left[1-e^{-\left(\frac{\alpha}{t}\right)}\right]^2\right]^\beta\right]^\zeta}{1+\left[1-\left[1-\left[1-e^{-\left(\frac{\alpha}{t}\right)}\right]^2\right]^\beta\right]^\zeta}, \tag{5}$$

and the associated pdf is defined as

$$f_{TIHLTLIE}\left(t;\zeta,\beta,\alpha\right)=\frac{4\zeta\beta\alpha t^{-2}e^{-\left(\frac{\alpha}{t}\right)}\left[1-e^{-\left(\frac{\alpha}{t}\right)}\right]\left[1-\left[1-e^{-\left(\frac{\alpha}{t}\right)}\right]^2\right]^{\beta-1}\left[1-\left[1-\left[1-e^{-\left(\frac{\alpha}{t}\right)}\right]^2\right]^\beta\right]^{\zeta-1}}{\left[1+\left[1-\left[1-\left[1-e^{-\left(\frac{\alpha}{t}\right)}\right]^2\right]^\beta\right]^\zeta\right]^2}, \tag{6}$$

For convenience, let

$$A(t)=1-e^{-\alpha/t},\ B(t)=1-A(t)^2,\ C(t)=1-B(t)^\beta \text{ and } D(t)=C(t)^\zeta \tag{7}$$

Then $$F_{TIHLTLIE}\left(t;\zeta,\beta,\alpha\right)=\frac{1-D(t)}{1+D(t)} \tag{8}$$

And the corresponding pdf is

$$f_{TIHLTLIE}\left(t;\zeta,\beta,\alpha\right)=\frac{4\zeta\beta\alpha t^{-2}e^{-\left(\frac{\alpha}{t}\right)}A\left(t\right)B\left(t\right)^{\beta-1}C\left(t\right)^{\zeta-1}}{\left(1+D(t)\right)^2} \tag{9}$$

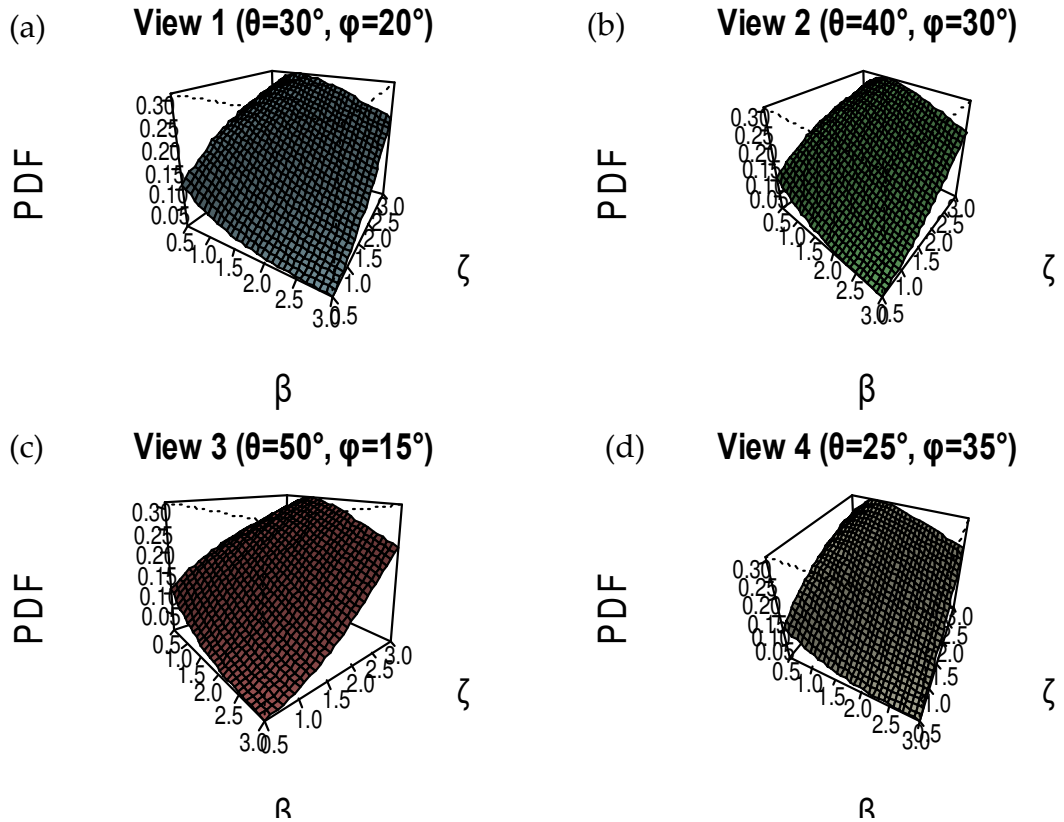


FIGURE 1 | 3D PDF surfaces of the TIHLTLIE distribution

The figure 1 above consists of plots which show the PDF as functions of the shape parameters ζ and β for fixed scale parameter α = 1.5 and time t = 2. Different viewing perspectives are presented: (a) θ=30°, φ=20°; (b) θ=40°, φ=30°; (c) θ=50°, φ=15°; (d) θ=25°, φ=35°.

2.1 | Linear Expansion

Considering the generalized binomial expansion,

$$\left(1+a\right)^{-d}=\sum_{q=0}^{\infty}\left(-1\right)^{q}\binom{d-1+q}{q}a^{q} \tag{10}$$

$$\left(1+a\right)^{d}=\sum_{q=0}^{\infty}\left(-1\right)^{q}\binom{d}{q}d^{q} \tag{11}$$

For $\left|a\right|<1$, and d being a positive real non-integer, the CDF and PDF of the TIHLTLIE distribution can be expanded.

Thus,

$$\left[H_{TIHLTLIE}\left(t;\zeta,\beta,\alpha\right)\right]^h=\left[1-\left[1-\left[1-\left[1-e^{-\left(\frac{\alpha}{t}\right)}\right]^2\right]^\beta\right]^\zeta\right]^h\left[1+\left[1-\left[1-\left[1-e^{-\left(\frac{\alpha}{t}\right)}\right]^2\right]^\beta\right]^\zeta\right]^{-h}$$

$$\left[H_{TIHLTLIE}\left(t;\zeta,\beta,\alpha\right)\right]^h=\sum_{i,j,k,l,m=0}^{\infty}\left(-1\right)^{i+j+k+l+m}\binom{h+1-i}{i}\binom{h}{j}\binom{\xi\left(i+j\right)}{k}\binom{\beta k}{l}\binom{2l}{m}e^{-\left(\frac{m\alpha}{t}\right)}$$

Therefore, $\left[H_{TIHLTLIE}\left(t;\zeta,\alpha,\lambda\right)\right]^h=\sum_{i=0}^{\infty}\rho_\omega e^{-\left(\frac{m\alpha}{t}\right)}$ (12)

Where $\rho_\omega=\sum_{j,k,l,m=0}^{\infty}\left(-1\right)^{i+j+k+l+m}\binom{h+1-i}{i}\binom{h}{j}\binom{\xi\left(i+j\right)}{k}\binom{\alpha k}{l}\binom{2l}{m}$

Likewise, considering pdf of the new TIHLTLIE model for expansion

$$f_{TIHLTLIE}\left(t;\zeta,\beta,\alpha\right)=4\zeta\beta\alpha t^{-2}e^{-\left(\frac{\alpha}{t}\right)}\left[1-e^{-\left(\frac{\alpha}{t}\right)}\right]\left[1-\left[1-e^{-\left(\frac{\alpha}{t}\right)}\right]^2\right]^{\beta-1}\left[1-\left[1-\left[1-e^{-\left(\frac{\alpha}{t}\right)}\right]^2\right]^\beta\right]^{\zeta-1}$$
$$\left[1+\left[1-\left[1-\left[1-e^{-\left(\frac{\alpha}{t}\right)}\right]^2\right]^\beta\right]^\zeta\right]^{-2}$$

The simple form of the pdf is expressed as

$$f_{TIHLTLIE}\left(t;\zeta,\beta,\alpha\right)=\sum_{n=0}^{\infty}\varphi_v\frac{e^{-\left(\frac{\alpha}{t}\right)}}{t^2}$$ (13)

where

$$\varphi_v=4\zeta\beta\alpha\sum_{p,q,r}^{\infty}\left(-1\right)^{n+p+q+r}\binom{1+n}{n}\binom{\xi n+\xi-1}{p}\binom{\beta p+\beta-1}{q}\binom{2q+1}{r}$$

2.2 | Mathematical Properties

The derivation of key mathematical properties of the proposed TIHLTLIE model is undertaken in this section.

2.2.1 | Probability Weighted Moments (PWMs)

The PWMs was introduced by Greenwood et al. (1979) as parameter estimation, alternative to convent

and distribution characterization. PWMs are particularly useful in deriving inverse-form estimators for both distributional parameters and quantiles. For a random variable *X*, the PWMs can be defined using the following general formulation..

$$M_{r,s} = E\left[t^r H\left(t\right)^s \right] = \int_{-\infty}^{\infty} t^r h\left(t\right)\left(H\left(t\right)\right)^s dt \tag{14}$$

To derive the PWMs of the TIHLTLIE distribution, Equations (8) and (9) are substituted into Equation (13), with the variable *h* replaced by *s* in the final expression.

$$M_{r,s} = \sum_{n,i,j=0}^{\infty} \rho_w \varphi_v \int_0^{\infty} t^{r-2} e^{-\left(\frac{m\alpha}{t}\right)2m} dt \tag{15}$$

The general form of the PWMs for the TIHLTLIE distribution is expressed as:

$$\sum_{n,i,j=0}^{\infty} \rho_w \varphi_v \left(2m\alpha\right)^{r-1} \Gamma\left(1-r\right) \tag{16}$$

Where φ_v and ρ_w are defined in (9) and (10)

2.2.2 | Moments

Using the expression in equation (9), the moment of the proposed TIHLTLIE distribution is

$$E\left(x^r\right) = \sum_{n=0}^{\infty} \int_0^{\infty} \varphi_v \left(2\lambda\right)^{r-1} \Gamma\left(1-r\right) \tag{17}$$

Where φ_v is defined in (12)

2.2.3 | Moment generating function

Similarly, the moment generating function is derived as

$$M_t^t = \sum_{n,w=0}^{\infty} \left(2\alpha\right)^w \frac{t^w \varphi_v}{w!} \Gamma\left(1-r\right) \tag{18}$$

Where φ_v is defined in (12)

2.2.4 | Reliability function

$$RH_{TIHLTLIE}\left(t;\zeta,\beta,\lambda\right) = 1 - F_{TIHLTLIE}\left(t;\zeta,\beta,\alpha\right) = \frac{2D\left(t\right)}{1+D\left(t\right)} \tag{19}$$

2.2.5 | Hazard function

$$A_{TIHLTLIE}(t,\zeta,\theta,\alpha)=\frac{f(t,\zeta,\beta,\alpha)}{E(t,\zeta,\beta,\alpha)}=\frac{2\zeta\beta\alpha\dfrac{e^{-\left(\frac{\alpha}{t}\right)}}{t^2}A(t)\left[B(t)\right]^{\beta-1}\left[C(t)\right]^{\zeta-1}}{\left[1+C(t)\right]^{\zeta}D(t)} \tag{20}$$

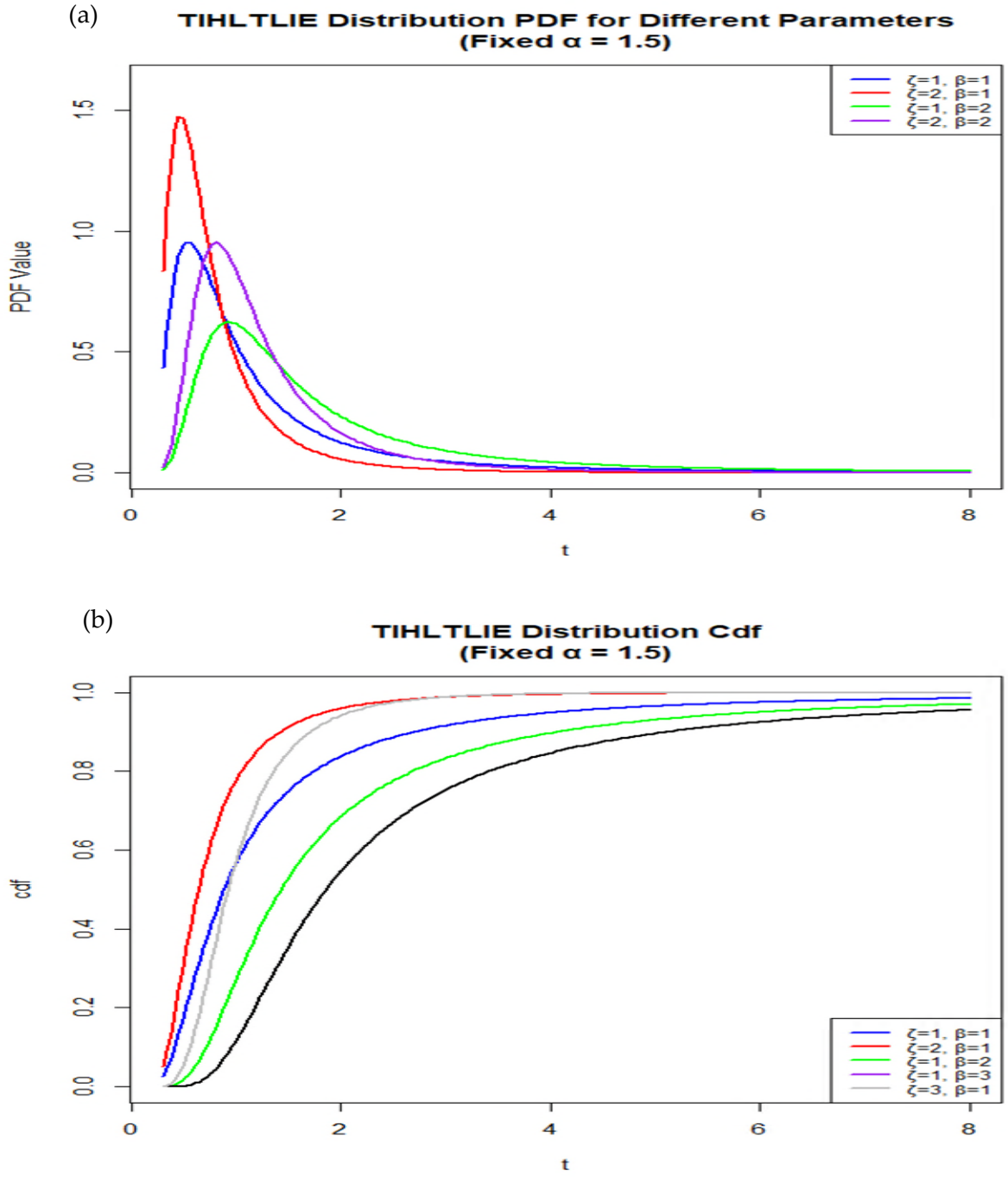


FIGURE 2 | 2D plots of ((a) PDF) and ((b) CDF) density curve of the TIHLTLIE distribution.

The figure 2 is the 2 dimensional plots of (a) PDF and (b) CDF for the proposed distribution with selected values of the shape parameters ζ and β and fixed scale parameter α = 1.5. These plots demonstrate the flexibility of the proposed distribution in capturing various density shapes, including right-skewed and heavy-tailed forms.

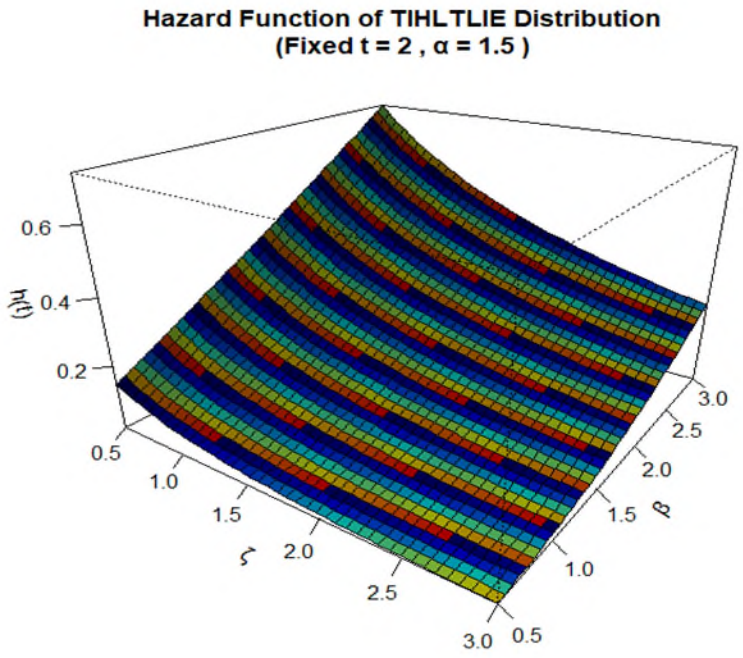


FIGURE 3 | Three-dimensional perspective plot of the TIHLTLIE distribution hazard rate function h(t) as a function of the shape parameters ζ and β.

From the figure 3 above, the plots demonstrates the flexibility of the proposed model in capturing various hazard shapes, including monotonic and non-monotonic failure rate patterns. The plot is generated at fixed time t = 2 and scale parameter α = 1.5..

2.2.6 Quantile function

$$T = Q(c) = -\frac{\alpha}{\ln\left[1-\left(1-\left(1-\left(\frac{1-c}{c+1}\right)^{1/\zeta}\right)^{1/\beta}\right)^{1/2}\right]} \tag{21}$$

2.2.7 Quantile Based on Bowley's Skewness and Moor's Kurtosis

We introduce quantile-based measures of skewness and kurtosis, namely Bowley's skewness and Moors' kurtosis. Using the quantile function defined in Equation (18), the corresponding expressions for Bowley's skewness and Moors' (1988) kurtosis are derived as follows

$$B = \frac{Q_{t0.75} - 2Q_{t0.50} + Q_{t0.25}}{Q_{t0.75} - Q_{t0.25}} \tag{22}$$

Moor's kurtosis M based on quantiles is expressed by

$$M = \frac{\left(Q_{t0.875} - Q_{t0.625}\right) + \left(Q_{t0.375} - Q_{t0.125}\right)}{\left(Q_{t0.75} - Q_{t0.25}\right)} \tag{23}$$

Particularly, $Q_{t0.25}$, $Q_{t0.50}$ and $Q_{t0.75}$ are the first, second and third quartiles of the TIHLTLIE distribution.

2.3 | Estimation Technique for Model Parameters

The $(\zeta, \beta, \alpha)^T$ represents the parameter vector and $x_{(1)} \le x_{(2)} \le \ldots \le x_{(n)}$ represents the ordered sample from the TIHLTLIE model with pdf and cdf represented by $f_{TIHLTLIE}\left(t;\zeta,\beta,\alpha\right)$ and $F_{TIHLTLIE}\left(t;\zeta,\beta,\alpha\right)$

2.3.1 | Maximum Likelihood Estimates (MLE)

The likelihood $L\left(\zeta,\beta,\alpha\right) = \prod_{i=1}^{n} f_{TIHLTLIE}\left(t;\zeta,\beta,\alpha\right) = \prod_{i=1}^{n}\left[\frac{4\zeta\beta\alpha t^{-2} e^{-\left(\frac{\alpha}{t}\right)} A\left(t\right) B\left(t\right)^{\beta-1} C\left(t\right)^{\zeta-1}}{\left(1+D(t)\right)^2}\right]$ (24)

The log-likelihood $\ell\left(\zeta,\beta,\alpha\right) = \sum_{i=1}^{n} In\left[\frac{4\zeta\beta\alpha t^{-2} e^{-\left(\frac{\alpha}{t}\right)} A\left(t\right) B\left(t\right)^{\beta-1} C\left(t\right)^{\zeta-1}}{\left(1+D(t)\right)^2}\right]$ (25)

The estimates satisfy the condition

$$\frac{\partial \ell}{\partial \zeta} = 0, \tag{26}$$

$$\frac{\partial \ell}{\partial \beta} = 0 \tag{27}$$

$$\frac{\partial \ell}{\partial \alpha} = 0 \tag{28}$$

the score equations is solved using numerical.

2.3.2 | Maximum Product of Spacing (MPS)

This method involved defining a spacing using the cdf of the ordered distribution: thus

$$D_i = F_{TIHLTLIE}\left(t_i;\zeta,\beta,\alpha\right) - F_{TIHLTLIE}\left(t_{i-1};\zeta,\beta,\alpha\right), \tag{29}$$

such that $D_i = F_{TIHLTLIE}\left(t_{(0)};\zeta,\beta,\alpha\right)=0, \quad F_{TIHLTLIE}\left(t_{(n+1)};\zeta,\beta,\alpha\right)=1$

Where $F_{TIHLTLIE}\left(t;\zeta,\beta,\alpha\right)=\frac{1-D(t)}{1+D(t)}$

Thus

$$D_i=\frac{1-D(t_{(i)})}{1+D(t_{(i)})}-\frac{1-D(t_{(i-1)})}{1+D(t_{(i-1)})} \tag{30}$$

The objective function is

$$N\left(\zeta,\beta,\alpha\right)=\frac{1}{n+1}\sum_{i=1}^{n+1}In\left(D_i\right) \tag{31}$$

Maximizing the estimates $N\left(\hat{\zeta},\hat{\beta},\hat{\alpha}\right)=\arg\max N(\zeta,\beta,\alpha)$

2.3.3 | Least Square Estimation (LS)

In the LS method, the empirical probabilities is defined as p_i such that $p_i=\frac{i}{n+1}$, then the objective function define as

$$LS\left(\zeta,\beta,\alpha\right)=\sum_{i=1}^{n}\left[F_{TIHLTLIE}\left(t_i;\zeta,\beta,\alpha\right)-p_i\right]^2 \tag{32}$$

$$LS\left(\zeta,\beta,\alpha\right)=\sum_{i=1}^{n}\left[\frac{1-D(t_{(i)})}{1+D(t_{(i)})}-\frac{i}{n+1}\right]^2 \tag{33}$$

Minimizing the $LS\left(\hat{\zeta},\hat{\beta},\hat{\alpha}\right)=\arg\min LS\left(\zeta,\beta,\alpha\right)$

2.3.4 | Weighted Least Square Estimation (WLS)

Consider the weight

$$w_i=\frac{\left(n+1\right)^2\left(n+2\right)}{i\left(n-i+1\right)}$$

The objective function

$$WLS\left(\zeta,\beta,\alpha\right)=\sum_{i=1}^{n}w_i\left[F_{TIHLTLIE}\left(t;\zeta,\beta,\alpha\right)-p_i\right]^2 \tag{34}$$

$$WLS\left(\zeta,\beta,\alpha\right)=\sum_{i=1}^{n}\frac{\left(n+1\right)^2\left(n+2\right)}{i\left(n-i+1\right)}\left[\frac{1-D(t_{(i)})}{1+D(t_{(i)})}-\frac{i}{n+1}\right]^2 \tag{35}$$

Minimizing $WLS\left(\hat{\zeta},\hat{\beta},\hat{\alpha}\right)=\arg\min WLS\left(\zeta,\beta,\alpha\right)$

2.3.5 | Cramér–von Mises Estimation (CVM)

$$CVM\left(\zeta,\beta,\alpha\right)=\frac{1}{12n}+\sum_{i=1}^{n}\left[F_{TIHLTLIE}\left[\left(t;\zeta,\beta,\alpha\right)\right]-\frac{2i-1}{2n}\right]^2 \tag{36}$$

$$CVM\left(\zeta,\beta,\alpha\right)=\frac{1}{12n}+\sum_{i=1}^{n}\left[\frac{1-D(t_{(i)})}{1+D(t_{(i)})}-\frac{2i-1}{2n}\right]^2 \tag{37}$$

Minimizing the $CVM\left(\zeta,\beta,\alpha\right)$

2.3.6 | Anderson–Darling Estimation (AD)

$$AD\left(\zeta,\beta,\alpha\right)=-n-\frac{1}{n}\sum_{i=1}^{n}\left(2i-1\right)\left[In\left(F_{TIHLTLIE}\left(t_{(i)};\zeta,\beta,\alpha\right)\right)+In\left(1-F_{TIHLTLIE}\left(t_{(n+1-i)};\zeta,\beta,\alpha\right)\right)\right] \tag{38}$$

By substitute the proposed model's cdf

$$AD\left(\zeta,\beta,\alpha\right)=-n-\frac{1}{n}\sum_{i=1}^{n}\left(2i-1\right)\left[In\left(\frac{1-D(t_{(i)})}{1+D(t_{(i)})}\right)+In\left(1-\frac{1-D(t_{((n+1-i))})}{1+D(t_{((n+1-i))})}\right)\right] \tag{39}$$

Minimizing $AD\left(\zeta,\beta,\alpha\right)$ will produce the estimate

2.3.7 | Percentile Estimation (PE)

This estimation method utilized the quantile of the distribution, employing the quantile of the proposed model in equation (21); thus,

$$Q\left(c\right)=-\frac{\alpha}{\ln\left[1-\left(1-\left(1-\left(\frac{1-c}{c+1}\right)^{1/\zeta}\right)^{1/\beta}\right)^{1/2}\right]}$$

Then the PE criterion becomes

$$PE\left(\zeta,\beta,\alpha\right)=\sum_{i=1}^{n}\left[t_{(i)}-Q\left(\frac{i}{n+1}\right)\right]^2 \tag{40}$$

2.3.8 | Method of Moments (MOM)

The moments of the proposed distribution denoted by $\mu_r^{'}$ is defined as

$$\mu_r^{'}=\int_0^{\infty}f_{TIHLTLIE}\left(t;\zeta,\beta,\alpha\right)dt \tag{41}$$

Therefore,

$$\mu_r^{'} = \int_0^{\infty} \frac{4\zeta\beta\alpha t^{-2} e^{-\left(\frac{\alpha}{t}\right)} A(t) B(t)^{\beta-1} C(t)^{\zeta-1}}{\left(1+D(t)\right)^2} dt \tag{42}$$

Set $m_r = \mu_r^{'}$ where $r = 1,2,3,...$
Note that $A(t), B(t), C(t)$ and $D(t)$ defined in equation (7)

2.3.9 | Probability Weighted Moments (PWM)

The concept of PWMs was introduced by Greenwood et al. (1979). Theoretically, the PWM is defined with respect to the proposed model as:

$$P_r = \int_0^{\infty} t\left[F_{TIHLTLIE}(t;\zeta,\beta,\alpha)\right]^r f_{TIHLTLIE}(t;\zeta,\beta,\alpha) dt \tag{43}$$

By substituting the cdf and the pdf,

$$P_r = \int_0^{\infty} t\left[\frac{1-D(t)}{1+D(t)}\right]^r \frac{4\zeta\beta\alpha t^{-2} e^{-\left(\frac{\alpha}{t}\right)} A(t) B(t)^{\beta-1} C(t)^{\zeta-1}}{\left(1+D(t)\right)^2} dt \tag{44}$$

2.3.10 | L-Moments (L-MOM)

Using the expression:

$$LM_1 = P_0 \tag{45}$$

$$LM_2 = 2P_1 - P_0 \tag{46}$$

$$LM_3 = 6P_2 - 6P_1 - P \tag{47}$$

Where each P_r represents the PWM of the proposed model

2.3.11 | Trimmed L-Moments (TL-MOM)

The population TL-Moments is defined with respect to the proposed model as:

$$P_r = \int_0^{\infty} t\left[F_{TIHLTLIE}(t;\zeta,\beta,\alpha)\right]^r f_{TIHLTLIE}(t;\zeta,\beta,\alpha) dt \tag{48}$$

By substituting the cdf and pdf terms, the TL-Moments are the solved numerically for the parameter ζ, β, α

2.3.12 | Energy Distance Estimation (ENE)

This method generate

$$Y_j = Q\left(U_j\right) \tag{49}$$

Where $Q(.)$ is the quantile function of the proposed model.

Then

$$ED\left(\zeta,\beta,\alpha\right) = \frac{2}{nm}\sum_{i=1}^{n}\sum_{j=1}^{m}|t_i - Y_j| - \frac{1}{m^2}\sum_{i=1}^{n}\sum_{j=1}^{m}|Y_j - Y_k| \tag{50}$$

Minimize $ED\left(\zeta,\beta,\alpha\right)$ to produce the estimates

2.3.13 | Wasserstein Distance Estimation (WDE)

Employing the proposed model quantile function, that is

$$Q\left(\frac{i}{n+1}\right) = -\frac{\alpha}{\ln\left[1-\left(1-\left(1-\left(\frac{1-c}{c+1}\right)^{1/\zeta}\right)^{1/\beta}\right)^{1/2}\right]}$$

The Wasserstein objective function is obtained as:

$$W_2\left(\zeta,\beta,\alpha\right) = \sum_{i=1}^{n}\left[t_{(i)} - Q\left(\frac{i}{n+1}\right)\right]^2 \tag{51}$$

and the resulting equation is solved by minimizing W_2

that is,

$$\hat{\zeta},\hat{\beta},\hat{\alpha} = \arg\min W_2$$

3.1 | Simulation Study

A simulation study was performed to evaluate the performance of the estimates of the proposed TIHLTLIE distribution via MLE, MPS, LS, WLS, CVM, AD, PE, MOM, L-MOM, PWM, WDE, TL-MOM, ENE methods. The study was conducted using 10,000 replications across various sample sizes: 15, 25, 100, 250, 500 and 1000.

Same parameter settings was considered: The three parameters were each set to 1.5
The simulation results corresponding to this setting is summarized in Table 1 to 6 below;

TABLE 1| Simulation Results of Estimators under Different Estimation Methods (n = 15)

N	Method	Estimates			Bias			MSE		
		ζ	β	α	ζ	β	α	ζ	β	α
15	MLE	1.9435	1.8126	1.6836	0.4435	0.3126	0.1836	0.9652	0.8125	0.5136
	MPS	1.4243	1.5575	1.5211	-0.0757	0.0575	0.0211	0.3657	0.5708	0.4000
	LS	1.5882	1.5652	1.5145	0.0882	0.0652	0.0145	0.6412	0.3555	0.2627
	WLS	1.6331	1.5945	1.5186	0.1331	0.0945	0.0186	0.6921	0.3849	0.2420
	CVM	1.9126	1.6959	1.627	0.4126	0.1959	0.1270	1.1713	0.5252	0.3963
	AD	1.7165	1.6135	1.5709	0.2165	0.1135	0.0709	0.6465	0.3502	0.2706
	PE	1.5882	1.5652	1.5145	0.0882	0.0652	0.0145	0.6412	0.3555	0.2627
	MOM	1.9735	1.8806	2.0257	0.4735	0.3806	0.5257	2.7888	0.6608	0.6966
	L-MOM	1.5575	1.5416	1.4950	0.0575	0.0416	-0.0050	0.0385	0.0145	0.0244
	PWM	1.5575	1.5416	1.4950	0.0575	0.0416	-0.0050	0.0385	0.0145	0.0244
	WDE	2.0171	1.6960	1.7842	0.5171	0.1960	0.2842	1.3127	0.7022	0.8218
	TL-MOM	1.5575	1.5416	1.4950	0.0575	0.0416	-0.0050	0.0385	0.0145	0.0244
	ENE	1.6760	1.5265	1.4242	0.1760	0.0265	-0.0758	0.0784	0.0200	0.0425

From the table 1, the PWM, L-MOM, and TL-MOM techniques provided estimates closest to the true parameter values while considering the lowest sample size, thereby exhibiting the smallest bias and MSE, followed by ENE with low estimation error. Contrarily, MOM, WDE, MLE, and CVM produced comparatively larger biases and MSEs, exhibiting poorer estimates

TABLE 2| Simulation Results of Estimators under Different Estimation Methods (n = 25)

N	Method	Estimates			Bias			MSE		
		ζ	β	α	ζ	β	α	ζ	β	α
25	MLE	1.7584	1.7012	1.6542	0.2584	0.2012	0.1542	0.4112	0.5551	0.3964
	MPS	1.4269	1.5266	1.5452	-0.0731	0.0266	0.0452	0.2116	0.4336	0.3413
	LS	1.5555	1.5528	1.5060	0.0555	0.0528	0.0060	0.3487	0.2369	0.1563
	WLS	1.5869	1.5769	1.5140	0.0869	0.0769	0.0140	0.3351	0.2156	0.1598
	CVM	1.7357	1.6258	1.5705	0.2357	0.1258	0.0705	0.5378	0.2819	0.2061
	AD	1.6303	1.5793	1.5462	0.1303	0.0793	0.0462	0.3268	0.2294	0.1555

	PE	1.5555	1.5528	1.5060	0.0555	0.0528	0.0060	0.3487	0.2369	0.1563
	MOM	1.4980	1.6706	1.7645	-0.0020	0.1706	0.2645	0.4718	0.1081	0.2586
	L-MOM	1.5682	1.5419	1.4928	0.0682	0.0419	-0.0072	0.0316	0.0112	0.0185
	PWM	1.5682	1.5419	1.4928	0.0682	0.0419	-0.0072	0.0316	0.0112	0.0185
	WDE	1.8848	1.5722	1.7802	0.3848	0.0722	0.2802	0.8226	0.4502	0.7075
	TL-MOM	1.5682	1.5419	1.4928	0.0682	0.0419	-0.0072	0.0316	0.0112	0.0185
	ENE	1.6398	1.5273	1.4465	0.1398	0.0273	-0.0535	0.0393	0.0119	0.0208

From table 2, at n = 25, all estimation techniques exhibited improved accuracy. PWM, L-MOM, and TL-MOM maintained their positions with consistently low bias and MSE, while ENE also exhibited strong comparative performance. MLE, WDE, and CVM still demonstrated poor comparative performance.

TABLE 3 | Simulation Results of Estimators under Different Estimation Methods (n = 100)

N	Method	Estimates			Bias			MSE		
		ζ	β	α	ζ	β	α	ζ	β	α
100	MLE	1.5550	1.6326	1.5371	0.0550	0.1326	0.0371	0.0610	0.2963	0.1713
	MPS	1.4541	1.5456	1.5212	-0.0459	0.0456	0.0212	0.0493	0.2568	0.1709
	LS	1.5103	1.5255	1.4995	0.0103	0.0255	-0.0005	0.0625	0.0702	0.0514
	WLS	1.5233	1.5382	1.5076	0.0233	0.0382	0.0076	0.0523	0.0793	0.0568
	CVM	1.5519	1.5466	1.5138	0.0519	0.0466	0.0138	0.0715	0.0756	0.0542
	AD	1.5268	1.5365	1.5100	0.0268	0.0365	0.0100	0.0504	0.0765	0.0553
	PE	1.5103	1.5255	1.4995	0.0103	0.0255	-0.0005	0.0625	0.0702	0.0514
	MOM	1.3639	1.5526	1.5225	-0.1361	0.0526	0.0225	0.0505	0.0217	0.0341
	L-MOM	1.5422	1.5396	1.5125	0.0422	0.0396	0.0125	0.0092	0.0070	0.0068
	PWM	1.5682	1.5419	1.4928	0.0682	0.0419	-0.0072	0.0316	0.0112	0.0185
	WDE	1.6296	1.4368	1.6866	0.1296	-0.0632	0.1866	0.2409	0.1446	0.4056
	TL-MOM	1.5422	1.5396	1.5125	0.0422	0.0396	0.0125	0.0092	0.0070	0.0068
	ENE	1.5852	1.5346	1.4892	0.0852	0.0346	-0.0108	0.0148	0.0065	0.0061

From table 3, considering moderate sample size of 100, the estimation accuracy improved substantially for all techniques. LS, WLS, CVM, AD, and PE also produced satisfactory results, while ENE pooled the lowest MSE, followed by L-MOM and TL-MOM however, MLE, MPS performance remained poor while WDE is poorer.

TABLE 4 | Simulation Results of Estimators under Different Estimation Methods (n = 250)

N	Method	Estimates			Bias			MSE		
		ζ	β	α	ζ	β	α	ζ	β	α

250	MLE	1.5198	1.5529	1.5310	0.0198	0.0529	0.0310	0.0221	0.1458	0.0938
	MPS	1.4764	1.4993	1.5359	-0.0236	-0.0007	0.0359	0.0212	0.1455	0.0963
	LS	1.5028	1.5073	1.5049	0.0028	0.0073	0.0049	0.0239	0.0314	0.0229
	WLS	1.5092	1.5151	1.5057	0.0092	0.0151	0.0057	0.0200	0.0328	0.0245
	CVM	1.5193	1.5175	1.5088	0.0193	0.0175	0.0088	0.0255	0.0322	0.0221
	AD	1.5083	1.5160	1.5050	0.0083	0.0160	0.0050	0.0192	0.0359	0.0228
	PE	1.5028	1.5073	1.5049	0.0028	0.0073	0.0049	0.0239	0.0314	0.0229
	MOM	1.4007	1.5368	1.5112	-0.0993	0.0368	0.0112	0.0295	0.0174	0.0236
	L-MOM	1.5357	1.5422	1.5107	0.0357	0.0422	0.0107	0.0046	0.0064	0.0044
	PWM	1.5422	1.5396	1.5125	0.0422	0.0396	0.0125	0.0092	0.0070	0.0068
	WDE	1.5712	1.4266	1.6372	0.0712	-0.0734	0.1372	0.1292	0.1099	0.2716
	TL-MOM	1.5357	1.5422	1.5107	0.0357	0.0422	0.0107	0.0046	0.0064	0.0044
	ENE	1.5543	1.5385	1.5006	0.0543	0.0385	0.0006	0.0060	0.0057	0.0033

From table 4, as the sample size increase to 250, almost all the estimators approached the true parameter values, while exhibiting great consistency. ENE retained the best overall performance with the lowest MSE consistently, followed by L-MOM and TL-MOM. MLE and MPS asymptotically improved, although, WDE continued to demonstrate comparatively poor performance.

TABLE 5 | Simulation Results of Estimators under Different Estimation Methods (n = 500)

N	Method	Estimates			Bias			MSE		
		ζ	β	α	ζ	β	α	ζ	β	α
500	MLE	1.5065	1.5369	1.5129	0.0065	0.0369	0.0129	0.0101	0.0939	0.0536
	MPS	1.4811	1.5040	1.5139	-0.0189	0.0040	0.0139	0.0097	0.0854	0.0516
	LS	1.4994	1.5069	1.4976	-0.0006	0.0069	-0.0024	0.0109	0.0154	0.0094
	WLS	1.5022	1.5053	1.5013	0.0022	0.0053	0.0013	0.0087	0.0154	0.0097
	CVM	1.5073	1.5110	1.5001	0.0073	0.0110	0.0001	0.0112	0.0149	0.0092
	AD	1.5012	1.5065	1.5000	0.0012	0.0065	0.0000	0.0086	0.0155	0.0098
	PE	1.4994	1.5069	1.4976	-0.0006	0.0069	-0.0024	0.0109	0.0154	0.0094
	MOM	1.4071	1.5287	1.4958	-0.0929	0.0287	-0.0042	0.0267	0.0183	0.0237
	L-MOM	1.5324	1.5381	1.5121	0.0324	0.0381	0.0121	0.0030	0.0060	0.0032
	PWM	1.5324	1.5381	1.5121	0.0324	0.0381	0.0121	0.0030	0.0060	0.0032
	WDE	1.5290	1.4751	1.5683	0.0290	-0.0249	0.0683	0.0862	0.1017	0.2144
	TL-MOM	1.5324	1.5381	1.5121	0.0324	0.0381	0.0121	0.0030	0.0060	0.0032
	ENE	1.5426	1.5371	1.5020	0.0426	0.0371	0.0020	0.0038	0.0055	0.0028

From table 5, at n = 500, the estimators converge greatly. While ENE demonstrated consistent smallest MSE, the L-MOM, PWM, and TL-MOM maintained smaller MSE. Traditional techniques such as MLE, LS, WLS, and AD also recorded improved estimation error, while WDE remained the highest MSE exhibiting lowest accuracy.

TABLE 6 | Simulation Results of Estimators under Different Estimation Methods (n = 1000)

N	Method	Estimates			Bias			MSE		
		ζ	β	α	ζ	β	α	ζ	β	α
1000	MLE	1.5030	1.5202	1.5056	0.0030	0.0202	0.0056	0.0054	0.0506	0.0310
	MPS	1.4892	1.4994	1.5082	-0.0108	-0.0006	0.0082	0.0049	0.0478	0.0294
	LS	1.4975	1.5069	1.4933	-0.0025	0.0069	-0.0067	0.0052	0.0069	0.0045
	WLS	1.5007	1.5025	1.4993	0.0007	0.0025	-0.0007	0.0040	0.0081	0.0052
	CVM	1.5017	1.5097	1.4943	0.0017	0.0097	-0.0057	0.0052	0.0071	0.0043
	AD	1.5007	1.5016	1.5001	0.0007	0.0016	0.0001	0.0040	0.0088	0.0057
	PE	1.4975	1.5069	1.4933	-0.0025	0.0069	-0.0067	0.0052	0.0069	0.0045
	MOM	1.4101	1.5913	1.4884	-0.0899	0.0913	-0.0116	0.0293	0.0275	0.0267
	L-MOM	1.5318	1.5345	1.5101	0.0318	0.0345	0.0101	0.0025	0.0055	0.0028
	PWM	1.5318	1.5345	1.5101	0.0318	0.0345	0.0101	0.0025	0.0055	0.0028
	WDE	1.5185	1.4839	1.5456	0.0185	-0.0161	0.0456	0.0620	0.0829	0.1652
	TL-MOM	1.5318	1.5345	1.5101	0.0318	0.0345	0.0101	0.0025	0.0055	0.0028
	ENE	1.5327	1.5327	1.5079	0.0327	0.0327	0.0079	0.0023	0.0049	0.0024

From table 6, as the sample size largely increased, all estimation techniques consistently stabilized, demonstrating their asymptotic property. ENE retained the best overall performance with the lowest MSE, followed by PWM, TL-MOM and L-MOM. MOM and WDE demonstrate poor comparative performance despite larger sample size.

TABLE 7 | MSE Results and Ranking Across Estimators (n = 15)

N	Method	MSE			Average Rank	Final Ranking
		ζ	β	α		
15	MLE	0.9652^{11}	0.8125^{13}	0.5136^{11}	11.67	11.5
	MPS	0.3657^{5}	0.5708^{10}	0.4000^{10}	8.33	9
	LS	$0.6412^{6.5}$	$0.3555^{6.5}$	$0.2627^{5.5}$	6.17	5.5
	WLS	0.6921^{8}	0.3849^{8}	0.2420^{4}	6.67	7
	CVM	1.1713^{12}	0.5252^{9}	0.3963^{9}	10.00	10
	AD	0.6465^{9}	0.3502^{5}	0.2706^{7}	7.00	8
	PE	$0.6412^{6.5}$	$0.3555^{6.5}$	$0.2627^{5.5}$	6.17	5.5

	MOM	2.7888^{13}	0.6608^{11}	0.6966^{12}	12.00	13
	L-MOM	0.0385^{2}	0.0145^{2}	0.0244^{2}	2.00	2
	PWM	0.0385^{2}	0.0145^{2}	0.0244^{2}	2.00	2
	WDE	1.3127^{10}	0.7022^{12}	0.8218^{13}	11.67	11.5
	TL-MOM	0.0385^{2}	0.0145^{2}	0.0244^{2}	2.00	2
	ENE	0.0784^{4}	0.0200^{4}	0.0425^{8}	5.33	4

From table 7, the ranking obviously confirms that L-MOM, PWM, and TL-MOM share the best-performing estimators for the initial small sample size, thereby begin with the highest ranking. While ENE ranked immediately after, whereas MLE, MOM, and WDE begin at the lowest positions.

TABLE 8 | MSE Results and Ranking Across Estimators (n = 25)

N	Method	MSE			Average Rank	Final Ranking
		ζ	β	α		
25	MLE	0.4112^{10}	0.5551^{13}	0.3964^{12}	11.67	12
	MPS	0.2116^{5}	0.4336^{11}	0.3413^{11}	9.00	10
	LS	$0.3487^{8.5}$	$0.2369^{8.5}$	$0.1563^{6.5}$	7.83	7.5
	WLS	0.3351^{7}	0.2156^{6}	0.1598^{8}	7.00	6
	CVM	0.5378^{12}	0.2819^{10}	0.2061^{9}	10.33	11
	AD	0.3268^{6}	0.2294^{7}	0.1555^{5}	6.00	5
	PE	$0.3487^{8.5}$	$0.2369^{8.5}$	$0.1563^{6.5}$	7.83	7.5
	MOM	0.4718^{11}	0.1081^{5}	0.2586^{10}	8.67	9
	L-MOM	0.0316^{2}	0.0112^{2}	0.0185^{2}	2.00	2
	PWM	0.0316^{2}	0.0112^{2}	0.0185^{2}	2.00	2
	WDE	0.8226^{13}	0.4502^{12}	0.7075^{13}	12.67	13
	TL-MOM	0.0316^{2}	0.0112^{2}	0.0185^{2}	2.00	2
	ENE	0.0393^{4}	0.0119^{4}	0.0208^{4}	4.00	4

From table 8, for n=25, L-MOM, PWM, and TL-MOM maintained their superiority performances, while ENE ranked next. AD, WLS, LS and PE demonstrated moderate rank, whereas WDE and MLE are poorly ranked

TABLE 9 | MSE Results and Ranking Across Estimators (n = 100)

N	Method	MSE			Average Rank	Final Ranking
		ζ	β	α		
100	MLE	0.0610^{9}	0.2963^{13}	0.1713^{12}	11.33	12
	MPS	0.0493^{5}	0.2568^{12}	0.1709^{11}	9.33	10

	LS	$0.0625^{10.5}$	$0.0702^{6.5}$	$0.0514^{6.5}$	7.83	6.5
	WLS	0.0523^{8}	0.0793^{10}	0.0568^{10}	9.33	10
	CVM	0.0715^{12}	0.0756^{8}	0.0542^{8}	9.33	10
	AD	0.0504^{6}	0.0765^{9}	0.0553^{9}	8.00	8
	PE	$0.0625^{10.5}$	$0.0702^{6.5}$	$0.0514^{6.5}$	7.83	7.5
	MOM	0.0505^{7}	0.0217^{5}	0.0341^{5}	5.67	5
	L-MOM	$0.0092^{1.5}$	$0.0070^{2.5}$	$0.0068^{2.5}$	2.17	2
	PWM	0.0316^{4}	0.0112^{4}	0.0185^{4}	4.00	4
	WDE	0.2409^{13}	0.1446^{11}	0.4056^{13}	12.33	13
	TL-MOM	$0.0092^{1.5}$	$0.0070^{2.5}$	$0.0068^{2.5}$	2.17	2
	ENE	0.0148^{3}	0.0065^{1}	0.0061^{1}	1.67	1

From table 9, at n = 100, ENE ranked best, followed by L-MOM and TL-MOM. PWM also performed well, while WDE ranked the poorest among its comparators

.

TABLE 10 | MSE Results and Ranking Across Estimators (n = 250)

N	Method	MSE			Average Rank	Final Ranking
		ζ	β	α		
250	MLE	$0.0221^{8.5}$	0.1458^{13}	0.0938^{11}	10.50	11
	MPS	0.0212^{7}	0.1455^{12}	0.0963^{12}	10.33	10
	LS	$0.0239^{10.5}$	$0.0314^{6.5}$	$0.0229^{7.5}$	8.17	8
	WLS	0.0200^{6}	0.0328^{9}	0.0245^{10}	8.33	9
	CVM	0.0255^{12}	0.0322^{8}	0.0221^{5}	8.33	9
	AD	0.0192^{5}	0.0359^{10}	0.0228^{6}	7.00	6
	PE	$0.0239^{10.5}$	$0.0314^{6.5}$	$0.0229^{7.5}$	8.17	8
	MOM	0.0295^{13}	0.0174^{5}	0.0236^{9}	9.00	9
	L-MOM	$0.0046^{1.5}$	$0.0064^{2.5}$	$0.0044^{2.5}$	2.17	2
	PWM	0.0092^{4}	0.0070^{4}	0.0068^{4}	4.00	4
	WDE	0.1292^{14}	0.1099^{11}	0.2716^{13}	12.67	13
	TL-MOM	$0.0046^{1.5}$	$0.0064^{2.5}$	$0.0044^{2.5}$	2.17	2
	ENE	0.0060^{3}	0.0057^{1}	0.0033^{1}	1.67	1

From table 10, ENE retained the most efficient estimator for larger samples and ranked first. L-MOM and TL-MOM retained second ranks, demonstrating their robustness as the most remaining techniques improved with increasing sample size, WDE retained rank worst

TABLE 11 | MSE Results and Ranking Across Estimators (n = 500)

N	Method	MSE	Average	Final

					Rank	Ranking
		ζ	β	α		
500	MLE	0.0101^{8}	0.0939^{12}	0.0536^{12}	10.67	11.5
	MPS	0.0097^{7}	0.0854^{11}	0.0516^{11}	9.67	10
	LS	$0.0109^{9.5}$	0.0154^{7}	$0.0094^{6.5}$	7.67	8
	WLS	0.0087^{6}	0.0154^{7}	0.0097^{8}	7.00	5.5
	CVM	0.0112^{11}	0.0149^{5}	0.0092^{5}	7.00	5.5
	AD	0.0086^{5}	0.0155^{9}	0.0098^{9}	7.67	8
	PE	$0.0109^{9.5}$	0.0154^{7}	$0.0094^{6.5}$	7.67	8
	MOM	0.0267^{12}	0.0183^{10}	0.0237^{10}	10.67	11.5
	L-MOM	0.0030^{2}	0.0060^{3}	0.0032^{3}	2.67	3
	PWM	0.0030^{2}	0.0060^{3}	0.0032^{3}	2.67	3
	WDE	0.0862^{13}	0.1017^{13}	0.2144^{13}	13.00	13
	TL-MOM	0.0030^{2}	0.0060^{3}	0.0032^{3}	2.67	3
	ENE	0.0038^{4}	0.0055^{1}	0.0028^{1}	2.00	1

From table 11, for n = 500, ENE maintained the first rank with the consistent lowest overall MSE. L-MOM, PWM, and TL-MOM ranked next. Conventional methods such as LS, WLS, CVM, and AD demonstrated satisfactory performance, while WDE remained the weakest.

TABLE 12 | MSE Results and Ranking Across Estimators (n = 1000)

N	Method	MSE			Average Rank	Final Ranking
		ζ	β	α		
1000	MLE	0.0054^{8}	0.0506^{12}	0.0310^{12}	10.67	12
	MPS	0.0049^{7}	0.0478^{11}	0.0294^{11}	9.67	10
	LS	0.0052^{9}	$0.0069^{5.5}$	$0.0045^{6.5}$	7.00	6
	WLS	$0.0040^{5.5}$	0.0081^{8}	0.0052^{8}	7.17	7
	CVM	0.0052^{9}	0.0071^{7}	0.0043^{5}	7.00	6
	AD	$0.0040^{5.5}$	0.0088^{9}	0.0057^{9}	7.83	8
	PE	0.0052^{9}	$0.0069^{5.5}$	$0.0045^{6.5}$	7.00	6
	MOM	0.0293^{12}	0.0275^{10}	0.0267^{10}	10.67	12
	L-MOM	0.0025^{3}	0.0055^{3}	0.0028^{3}	3.00	3
	PWM	0.0025^{3}	0.0055^{3}	0.0028^{3}	3.00	3
	WDE	0.0620^{13}	0.0829^{13}	0.1652^{13}	13.00	13
	TL-MOM	0.0025^{3}	0.0055^{3}	0.0028^{3}	3.00	3
	ENE	0.0023^{1}	0.0049^{1}	0.0024^{1}	1.00	1

From table 12, at the highest sample size, ENE emerged the best overall ranking, exhibiting its superiority in efficiency and consistency. L-MOM, PWM, and TL-MOM remained second rankings revealing it comparative efficiency and consistency. Despite the asymptotic properties enjoyed by all techniques, WDE and MOM continued to demonstrate poorest rankings, indicating relatively lower estimation efficiency.

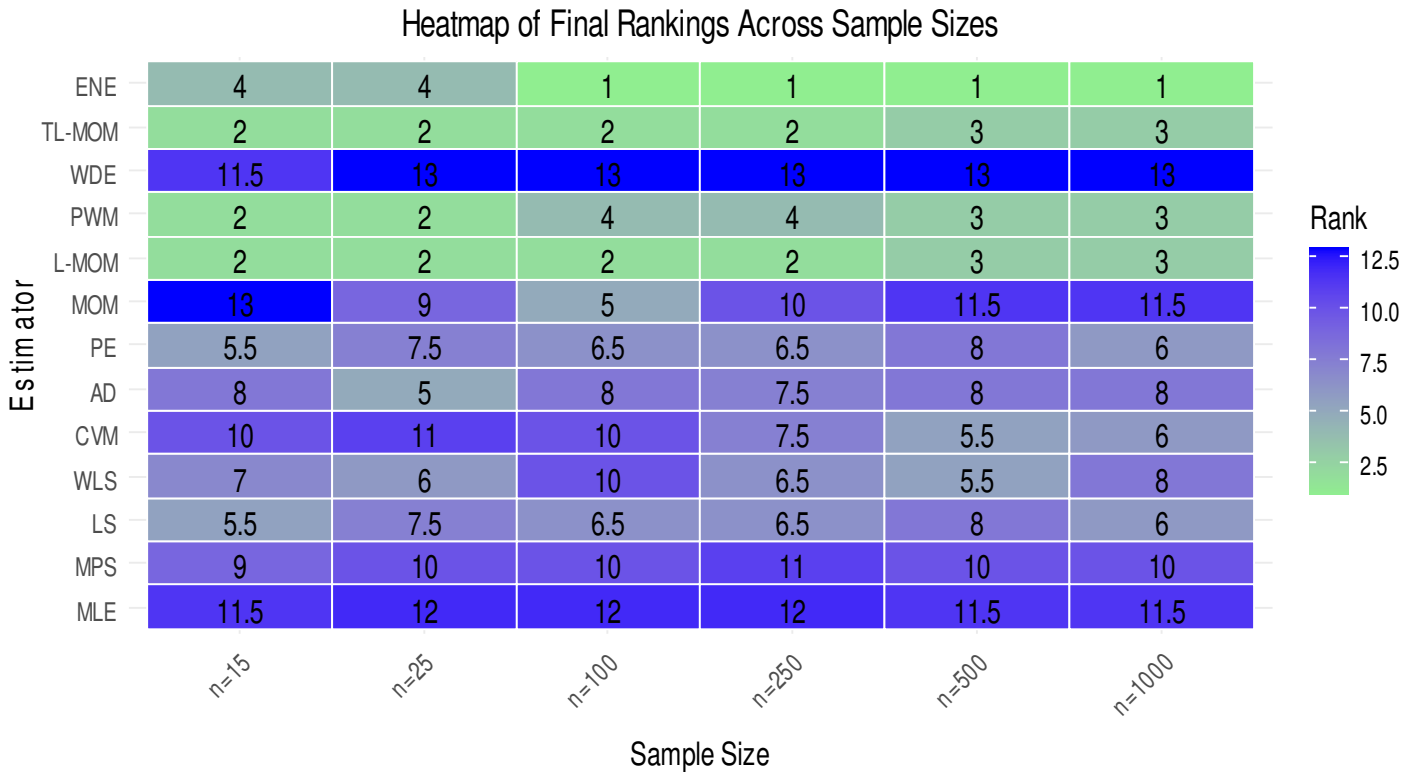


FIGURE 4| Comparative Heatmap of Final Rankings for Competing Estimation Techniques Across Sample Sizes.

The figure 4 is a comparative heatmap Ranking which reveals the performance through rank across the distinct sample sizes. From this figure, it is obvious that the ENE method was among the best four techniques at n<100, and became the highest ranking at n>100. TL-MOM and L-MOM are other alternative.

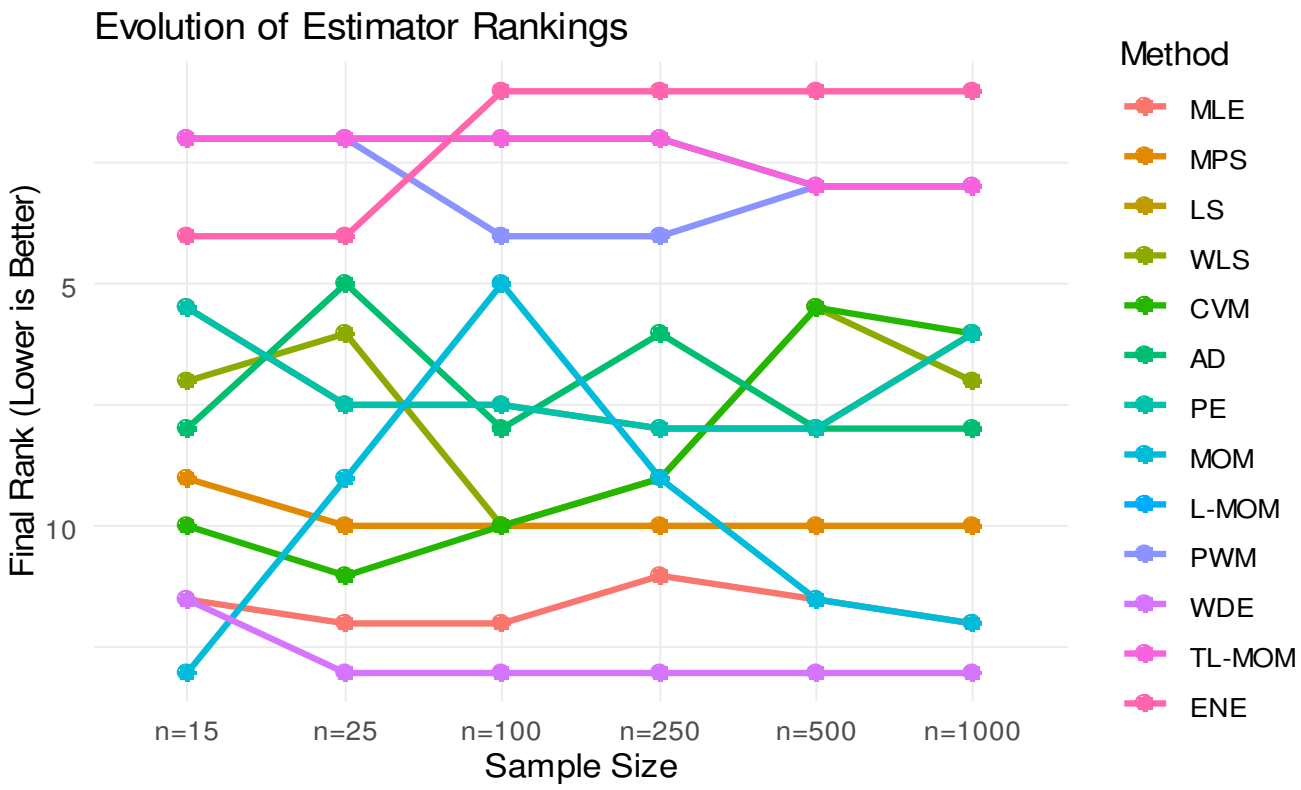


FIGURE 5 | Overall Performance Comparison of Estimation techniques Based on Average Final Rankings

From figure 5, the overall performance comparison of all the distinct estimation techniques based on the final ranking across the sample sizes is revealed. This figure is important as it shows how each and every technique employed in this study evolved. Due to ties in rank among the techniques, for instance at n=15, TL-MOM, PWM and L-MOM are the same line, PE and LS are the same line and WDE and MLE are the same line. Same applies across the other sample sizes. The techniques with the lowest ranking can be easily identified and considered as the best techniques.

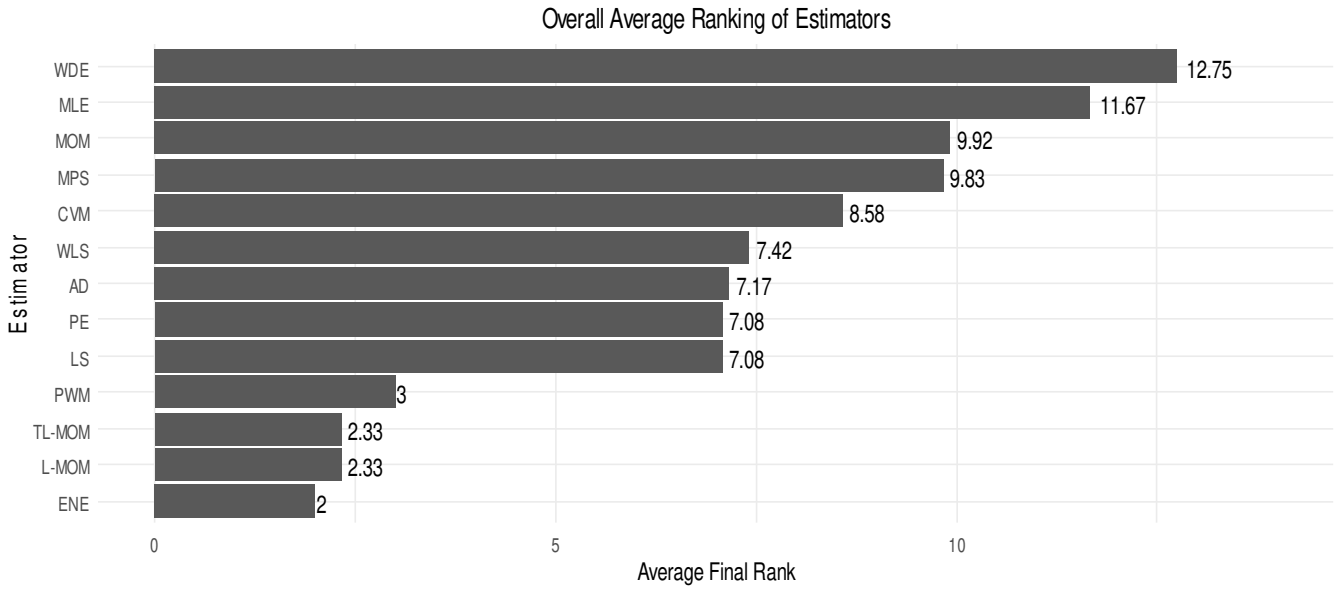


FIGURE 6 | Overall Average Ranking of the Estimation Techniques

The figure 6 reveals the overall average ranking of the estimation techniques computed from the final rankings across all sample sizes. The smaller average ranks correspond to better overall performance

3.2 Discussion of the Ranking Results Across Sample Sizes

Tables corresponding to sample sizes n=15,25,100,250,500, and 1000 summarize the relative performance of the thirteen estimation procedures based on parameter-specific MSE rankings, average ranks, and overall rankings. Since smaller MSE values indicate greater estimation accuracy, methods with lower average ranks are considered superior.

The L-MOM, PWM, and TL-MOM estimators jointly dominate the leading position with an average rank of 2.00 when considering smallest sample size (n = 15). This output demonstrating remarkable stability in greatly small sample size, follow by the Energy Distance Estimator (ENE) with a final rank of 4, while LS and PE level up at moderate performance leaving behind the MPS, WLS and AD at a close distance. In contrast, MLE, MOM, and WDE demonstrate the weakest performance, indicating substantial estimation variability under great data scarcity.

At n = 25, a similar demonstration evolves. The L-moment-based estimators continue to dominate with a final rank of 2, follow by the ENE method which indicates high competition and ranked fourth position. Classical estimators such as MLE, CVM, and WDE continue to occupy the lower end of the ranking spectrum, suggesting that their efficiency remains poor in small-to-moderate samples. While AD, WLS and MOM improved.

For n = 100, a remarkable drift unveils. The ENE estimator becomes competitive and attained best-performing technique, securing the overall first position, through the smallest average rank of 1.67. L-MOM and TL-MOM remain greatly competitive with a second position,, while PWM drops to fourth ranks. This result i that distance-based estimation gains efficiency more rapidly than other classical techniques as additional information made available.

As the sample size increases to n = 250, the ENE becomes more superior, retaining the top overall rank. L-MOM and TL-MOM continue to occupy final rank of 2 whereas PWM retains fourth ranks. Among the conventional techniques, AD happens to be the strongest in term of performance over, MPS, MLE, LS, CVM, WLS and MOM. WDE consistently remains the weakest ranking, indicating that the Wasserstein criterion may be less suitable for the TIHLTLIE distributional structure.

In addition, n = 500 further validate these results. ENE remains the best overall ranking, The L-moment-based estimators pulled the next ranking. Followed by other classical methods, while, WDE remain the poorest technique.

Lastly, at n=1000, ENE achieves impeccable performance, overwhelmingly dominating the other methods by obtaining average ranking of one for all three parameters and an overall ranking 1. L-MOM, PWM, and TL-MOM retain the second-best group, confirming their consistency and robustness even at very large sample sizes. Methods such as PE, LS, CVM, WLS, and AD show incredible performance but could not match the efficiency of ENE and the L-moment family. MOM, MLE, and WDE remain the poorest, indicating comparatively slower convergence and reduced finite-sample efficiency for the TIHLTLIE distribution.

Overall, the simulation study demonstrates three major patterns. First, estimation accuracy improves as the sample size increases, evidenced by the substantial reduction in MSE values across all techniques. Second, L-moment-based estimators (PWM, L-MOM, and TL-MOM) demonstrate exceptional performance in small samples, making them attractive choices when small sample sizes are available. Third, the Energy Distance Estimator emerges as the most efficient estimator in moderate and large samples, achieving the best overall rankings from n = 100 and above and consistently produces the smallest MSE values. These findings suggest that ENE remains the most reliable estimation method for the TIHLTLIE distribution, while L-moment-based methods remain an excellent choice in small-sample sizes

3.2 | Applications

This section introduced the dataset (breaking stress of carbon fibers) explored in this study, the dataset consist of 100 observations extracted from article by Nichols and Padgett (2006). The dataset was truncated and 50 observations were modeled via the proposed model alongside with the competing

models. Descriptive statistics of the two datasets were provided. The estimates of the models parameters and the outcome of various information criteria were produced.

TABLE 13 | Summary of the two datasets

Dataset	Min.	Skewness	Median	Mean	Mode	Variance	Kurtosis	Max.
I	0.39	0.98013	1.945	2.2926	1.5	1.44822	0.27664	5.56
II	1.47	0.41216	2.94	2.9502	2.75	0.40806	1.19259	4.9

From table 13, the descriptive statistics reveal that both datasets are positively skewed, with dataset I showcasing more skewness and variability compared to dataset II. Higher mean, median and kurtosis exhibited in dataset II indicating larger observations on average and more peaked distribution

TABLE 14 | Estimates of TIHLTLIE and Information criteria measure for the fitted models based on dataset I

Models	MLE			AIC	BIC	CAIC	HQIC
TIHLTLIE	1.5138	1.7214	1.7675	180.2996	186.0356	180.8213	182.4839
TLOLLIE	0.9576	1.7280	0.6594	341.5254	347.2615	342.0471	343.7097
WWIE	0.2645	1.9702	0.9643	193.8873	199.6234	194.4091	196.0717
GoIE	1.0617	0.9576	0.5954	271.9906	272.5124	277.7267	274.1750

From the table 14, the dataset I, the proposed model provides the best fit as evidenced by the lowest AIC, BIC, CAIC and HQIC values among the comparators, indicating the dominance of the TIHLTLIE model against TLOLLIE, WWIE and GoIE models.

TABLE 15 | Estimates of TIHLTLIE and Information criteria measure for the fitted models based on dataset II

Models	MLE			AIC	BIC	CAIC	HQIC
TIHLTLIE	1.9353	1.8960	1.7242	156.1503	161.8863	156.672	158.3346
TLOLLIE	0.8583	0.1053	0.7813	569.9098	575.6459	570.4316	572.0942
WWIE	0.1993	0.3927	0.4748	716.4375	722.1735	716.9592	718.6218
GoIE	0.7797	1.5999	1.4663	158.3533	164.0894	158.8750	160.5376

Similarly, from the table 15, the dataset II**,** the proposed model provides the best fit as evidenced by the lowest AIC, BIC, CAIC and HQIC values among the comparators, indicating the dominance of the TIHLTLIE model against TLOLLIE, WWIE and GoIE models.

Table 16 | Breaking Stress of Carbon Fibers Data

(a) Data set I

2.81, 2.77, 2.17, 2.83, 1.92, 3.70, 2.74, 2.73, 1.47, 3.11, 4.42, 2.41, 3.19, 2.50, 3.60, 3.11, 3.27, 2.87, 3.22,1.69,3.28, 3.09, 1.87, 3.15, 4.90, 3.75, 2.43, 2.95, 2.97, 3.39, 2.96, 2.53, 2.67, 20, 3.33, 2.55, 3.31, 3.31, 2.85, 2.56, 3.56, 3.15, 2.35, 2.55, 2.59, 2.38, 2.93, 3.22,3.39, 2.81, 4.

(b) Data set II

1.84, 1.59, 3.19, 1.57, 1.41, 3.68, 2.97, 1.36, 0.98, 2.76, 4.91, 3.68, 0.81, 5.56, 1.73,1 2.17, 1.17, 5.08, 2.48, 1.18, 3.51, 2.17, 1.69, 0.85, 1.61, 2.79, 4.70, 2.03, 1.80, 1.57, 1.08, 2.03, 1.61, 2.12,1.89, 2.88, 2.82, 1.25, 4.38,1.84, 0.39, 3.68, 2.48, 2.05, 3.65, .59, 2.00, 1.22, 1.12, 1.71.

From the table 16, the two datasets ((a) and (b)), each consist of 50 observations of breaking stress of carbon fibers which can be found in the article written by [6]

4 | Conclusion

This study introduced the TIHLTLIE distribution, a new and flexible lifetime model capable of accommodating a wide range of data behaviors encountered in reliability, survival, and applied statistical analyses. Fundamental distributional properties, such as the moments, probability weighted moments, moment generating function quantile function, survival measures, and hazard rate function, were derived and examined. The three dimensional and two dimensional visualizations of the density and hazard function demonstrated that the proposed model is capable of modeling diverse shapes, including right-skewed, nearly symmetric, and heavy-tailed patterns, indicating its adaptability to different dimensional data structures.

To facilitate practical implementation of the new model, parameter estimation was explored via extensive set of estimation methods comprising MLE, MPS, LS, WLS, CVM, AD, PE, MOM, L-MOM, PWM, TL-MOM, WDE, and ENE. Extensive Monte Carlo simulation study was carried out to investigate the finite-sample performance of these estimators under varying sample sizes. The results showed that the accuracy of the all estimators is impeccable as the sample size increased, confirming their asymptotic properties. However, the ENE and the moment-based methods, particularly PWM, L-MOM, and TL-MOM, proved to be the most accurate and stable parameter estimates, while MLE and several classical minimum-distance methods exhibited comparatively larger estimation errors in smaller samples.

The practical applicability of the TIHLTLIE distribution was further demonstrated using real-world datasets. Exploring AIC, BIC, CAIC, and HQIC, the standard model selection criteria, the new distribution consistently proved its competitive advantage against the existing alternative models, underscoring the robustness, flexibility, and applicability of the TIHLTLIE distribution for modeling positively skewed lifetime data.

Overall, the new model has demonstrated how it can enriches the family of inverted lifetime models and offers a strategic alternative for statistical modeling in reliability engineering, Future investigations may consider extending the TIHLTLIE distribution to statistical process monitoring applications, regression frameworks, censored data settings and copula-based dependence modeling. **Data Availability**

Author Contributions

Conceptualization: AAA, ZFA. Methodology: AAA, AAI .Software: AAI, BOA, HA. Validation: ZFA, AAA, AAI. Formal Analysis: AAA, BOA. Investigation: HA, ZFA .Resources: AAA, HA. Data Curation: AAA, AAI. Writing- original draft preparation: AAA, HA. Visualization: AAI, BOA. Supervision: AAI, BOA, AAA. Project administration: AAI, BOA, AAA. Funding acquisition: ZFA, AAA, HA.

Acknowledgements:

The authors would like to thank Princess Nourah bint Abdulrahman University Researchers Supporting Project number (PNURSP2026R913), Princess Nourah bint Abdulrahman University, Riyadh, Saudi Arabia.

Funding Statement:

The authors express their gratitude to Princess Nourah bint Abdulrahman University Researchers Supporting Project number (PNURSP2026R913), Princess Nourah bint Abdulrahman University, Riyadh, Saudi Arabia.

Disclosure

All authors have read and agreed to the publication of this manuscript.

Conflicts of Interest

The authors declared no conflicts of interest.

Data Availability Statement

All datasets used are included in the paper.

References

[1] Eliwa, M.S.; Altun, E.; Alhussain, Z.A.; Ahmed, E.A.; Salah, M.M.; Ahmed, H.H.; El-Morshedy, M. A new one-parameter lifetime distribution and its regression model with applications. PLoS ONE 2021, 16, e0246969.

[2] El-Morshedy, M.; Alshammari, F.S.; Hamed, Y.S.; Eliwa, M.S.; Yousof, H.M. A New Family of Continuous Probability Distributions. Entropy 2021, 23, 194.

[3] Yousof, H.M.; Altun, E.; Ramires, T.G.; Alizadeh, M.; Rasekhi, M. A new family of distributions with properties, regression models and applications. J. Stat. Manag. Syst. 2018, 21, 163–188.

[4] Isa A. M., Sule O. B., Ali B. A., Akeem A. A., and Ibrahim I. I. (2022). Sine-Exponential Distribution: Its Mathematical Properties and Application to Real Dataset. UMYU Scientifica, 1(1), 127 – 131.

[5] Adepoju, A. A., Abdulkadir, S. S., & Jibasen, D. (2023). The Type I Half Logistics-Topp-Leone-G Distribution Family: Model, its Properties and Applications. UMYU Scientifica, 2(4), 09-22.

[6] Abonongo A. I. L., Abonongo J. (2024). Exponentiated Generalized Weibull Exponential distribution: Properties and applications. Computational Journal of Mathematical and Statistical Sciences. 3(1), 57-84.

[7] Adetunji A. A., Sabri S. R. M. (2024). A new two-parameter poisson-transmuted exponential distribution: Properties and applications in count observation. AIP Conference proceedings 3016(1).

[8] Radwan H., Ghazal M. M. M, (2024) Modified Generalized Linear Exponential Distribution: Properties and Applications. Statistics, Optimization and information computing, 12(1), 231-255.

[9] Adepoju, A. A., Abdulkadir, S. S., & Jibasen, D. (2024). On Different Classical Estimation Approaches for Type I Half Logistic-Topp-leone- Exponential Distribution. RT&A, No 1 (77) Volume 19.

[10] Lemonte, A. J. (2013). A new exponential-type distribution with constant, decreasing, increasing, upside-down bathtub and bathtub-shaped failure rate function. Computational Statistics Data Analysis, 62: 149-170.

[11] Keller A. Z., Kamath A. R., (1982). Reliability analysis of cnc machine tools. Reliability Engineering, 3: 449-473.

[12] Sule O. B. (2023). A study on the properties of a new exponentiated extended Inverse Exponential distribution with applications. RT & A, No 3(74).

[13] Abbas S., Mustafa F., Taqi S. A., Cakmakyapan S., Ozel G (2020). A Note on Topp-Leone Odd Log-Logistic Inverse Exponential Distribution. Journal of Statistical Theory and Applications, Vol. 19(3), pp.

[14] Oguntunde P., Khaleel M., Opanuga H. O. A., Owolabi F. (2018) The gompertz Inverse Exponetial distribution with applications. Cogent Mathematics & Statistics, 5:1.

[15] Alshahrani M.N. (2023). Weighted Weibull Inverse Exponential Model with Application. Advances and Applications in Statistics. Volume 89, Number 1, 2023, Pages 55-72.

[16] Adepoju A. A., Abdulkadir S. S., Jibasen D., Olumoh J. S. (2024). Type I Half Logistic Topp-leone Inverse Lomax Distribution with Applications in Skinfolds Analysis. Reliability: Theory & Applications. 1(77), 618-630. https://doi.org/10.24412/1932-2321-2024-177-618-630

[17] Isa A. M., Kaigama A., Adepoju A. A., Bashiru S. O., Lehmann Type II-Lomax Distribution: Properties and Application to Real Data Set. (2023). Communication in Physical Sciences, 9(1):63 – 72

[18] Abdulrahman A. T., Alshawarbeh E., and Abd El-Raouf M. M., (2023)."Statistical Modeling Using a New Distribution with Application in Health Data," Mathematics, vol. 11, no. 14, p. 3108.

[19] Alamri O. A., Alessa A. H., Hussam E., Alhelali M. H., Kilai M. (2023). "Statistical modelling for the Covid-19 mortality rate in the Kingdom of Saudi Arabia," Alexandria Engineering Journal, vol. 68, pp. 517-526,

[20] Adepoju, A. A., Isa, A. M., Bello, O. A. Cosine Marshal-Olkin-G Family of Distribution: Properties and Applications. (2024b). Reliability: Theory & Applications. 3(79): 408-422, DOI: https://doi.org/10.24412/1932-2321-2024-379-408-422

[21] Adepoju, A. A. ., Elbarkawy, M. A. F. ., Ishaq, A. I. ., Sawaran Singh, N. S. ., Daud, H. ., Suleiman, A. A. ., Almetwally, E. M. ., & Elgarhy, M. . (2025). A Flexible Extension of the Log-Logistic Distribution with Application to Cancer Data . International Journal of Statistics in Medical Research, 14, 626–642. https://doi.org/10.6000/1929-6029.2025.14.59.

[22] Panitanarak, U., Ishaq, A. I., Sawaran Singh, N. S., Usman, A., Usman, A. U., Daud, H., Adepoju, A. A., Sadiq, I. A., & Suleiman, A. A. (2025). Machine Learning Models in Predicting Failure Times Data Using a Novel Version of the Maxwell Model. European Journal of Statistics, 5, Article 1. https://doi.org/10.28924/ada/stat.5.1.

[23] Khalaf, A. A., Khaleel, M. A., Mazarei, D., Tolba, A. H., & Adepoju, A. A. (2025). Evaluating the performance of Bayesian estimates for Burr XII Inverse Rayleigh parameters using MCMC. Iraqi Statisticians Journal, 2(2), 49–63.

[24] Adepoju A. A., Bello A. O., Isa A. M., Adesupo A., & Olumoh J. S. (2024d). Statistical inference on sine-exponential distribution parameter. Journal of Computational Innovation and Analytics, 3(2), 129-145. https://doi.org/10.32890/jcia2024.3.2.6

[25] Adepoju A. A, Mohammed U, Sani S. S, Adamu K, Tukur K, Ishaq A. I. Statistical Properties of Negative Binomial Distribution under Imprecise Observation. (2019). Journal of the Nigerian Statistical Association. 31, 289-294.

[26] Nicholas M. D. , Padgett W. J.(2006). A bootstrap control chat for Weibull percentile. Quality and Reliability engineering international, 22:141-151.